

The luminosity dependence of clustering and higher order correlations in the PSCz survey

István Szapudi^{1,2}, Enzo Branchini³, C. S. Frenk¹, Steve Maddox⁴, Will Saunders⁵

¹ *Department of Physics, University of Durham, South Road, Durham DH1 3LE, UK*

² *CITA, University of Toronto, 60 George Street, Ontario, Canada, M5S 3H8 (present address)*

³ *Kapteyn Institute, University of Groningen, Landleven 12, Groningen, 9700 AV, the Netherlands*

⁴ *School of Physics and Astronomy, University of Nottingham, Nottingham NG7 2RD* ⁵ *Institute for Astronomy, Blackford Hill, Edinburgh EH9 9RJ, UK*

29 October 2018

ABSTRACT

We investigate the spatial clustering of galaxies in the PSCz galaxy redshift survey, as revealed by the two-point correlation function, the luminosity mark correlations, and the moments of counts-in-cells. We construct volume-limited subsamples at different depths, and search for a luminosity dependence of the clustering pattern. We find no statistically significant effect in either the two-point correlation function or the mark correlations and so we take each subsample (of different characteristic luminosity) as representing the same statistical process. We then carry out a counts-in-cells analysis of the volume-limited subsamples, including a rigorous error calculation based on the recent theory of Szapudi, Colombi and Bernardeau. In this way, we derive the best estimates to date of the skewness and kurtosis of IRAS galaxies in redshift space. Our results agree well with previous measurements in both the parent angular catalogue, and in the derived redshift surveys. This is in contrast with smaller, optically selected surveys, where there is a discrepancy between the redshift space and projected measurements. Predictions from cold dark matter theory, obtained using the recent semi-analytical model of galaxy formation of Benson *et al.*, provide an excellent description of our clustering data.

Key words: large scale structure of the universe — methods: numerical

1 INTRODUCTION

The clustering pattern of galaxies observed today reflects an interplay between two fundamental processes: the gravitational growth of primordial density fluctuations and the physics of galaxy formation. In general, we expect the process of galaxy formation to segregate the galaxies from the underlying dark matter distribution and even to give rise to dependencies of clustering on physical properties, such as galaxy colour, luminosity, morphological type or star formation rate (e.g., Kauffmann *et al.* 1999, Benson *et al.* 2000). Such segregation is usually referred to as “biasing.”

Biasing was originally introduced as a useful device to match theoretical predictions for the distribution of cold dark matter (CDM) with observations of the spatial correlations of clusters and galaxies (Kaiser 1984, Davis *et al.* 1985, Bardeen *et al.* 1986). Since then, the statistical properties of the dark matter distribution in CDM models has been extensively investigated by means of N-body simulations (e.g. Jenkins *et al.* 1998, Gross *et al.* 1999). Observationally, how-

ever, little is known about the large-scale distribution of dark matter, although this situation may soon change as gravitational lensing techniques become increasingly sensitive (Fischer *et al.* 2000). In the meantime, partial information on biasing may be obtained by studying the relative clustering of galaxies with different physical characteristics. This, in turn, requires large surveys like the one we analyze in this paper.

The simplest statistical tool to quantify clustering is the two-point correlation function, defined as the excess probability above (or below) random that an object be found at a certain separation from another, randomly chosen object. Two-point statistics completely describe a Gaussian point process. However, the galaxy distribution is patently non-Gaussian, as evidenced, for example, by the presence of rich clusters and walls. A natural generalization is the complete set of N -point correlation functions which provide a full characterization of a distribution. Unfortunately, their measurement and interpretation become exponentially dif-

difficult as the order, N , increases. This is why counts-in-cells analysis, which extracts the *average* of the N -point correlation functions over a cell, has become the most practical and popular tool for describing higher order clustering in the galaxy distribution (e.g., Peebles 1980, Efstathiou *et al.* 1991, Bouchet *et al.* 1993, Szapudi, Meiksin, & Nichol 1996, Gaztañaga 1994, Szapudi & Szalay 1997, Szapudi, & Gaztañaga 1998).

This paper calculates two-point statistics and presents a counts-in-cells analysis of the PSCz survey of IRAS galaxies (Saunders *et al.* 2000). Our analysis is motivated, in part, by a desire to characterize some of the possible manifestations of biasing, such as a dependency of clustering on luminosity or a particular functional form for high order statistics. To this aim, we construct volume-limited catalogues from the PSCz survey which provide a controlled, homogeneous framework for statistical analysis. The most efficient tool to search for a luminosity dependence of clustering is the luminosity mark correlation (Beisbart and Kerscher 2000) which we apply to the PSCz. We also compare our measurements with a model of galaxy formation in the context of the CDM cosmology (Benson *et al.* 2000) which makes specific predictions for the statistics that we investigate. A previous search for luminosity effects in the clustering of IRAS galaxies, based on the QDOT survey, failed to reveal any signal (Moore *et al.* 1994). However, a preliminary analysis of the PSCz survey (Maddox *et al.* 2000) suggests that some effect could well be present.

The rest of this paper is organized as follows. In §2, we present brief details of the dataset and describe our measurements of the two-point correlation function, mark correlations, and the moments of counts-in-cells up to fourth order. In §3, we compare our estimates with measurements for other surveys, both optical and infrared, and with the prediction of the Benson *et al.* model.

2 DATASET AND MEASUREMENTS

In this section, we characterize the clustering of galaxies in the PSCz redshift survey using three complementary descriptors: the two-point correlation function (§2.2), the mark correlations (§2.3), and the higher order correlation amplitudes or cumulants, the skewness and kurtosis (§2.4). All three statistics were calculated for a series of volume-limited subsamples, each containing all PSCz galaxies in spheres of radius 50, 75, 100, 125, 150, 175, and $200h^{-1}$ Mpc, namely 1160, 2159, 2189, 1985, 1671, 1456, and 1259 galaxies, respectively. We chose to work with volume-limited subsamples because these are homogeneous catalogues that are simple to treat statistically and, as shown by Colombi, Szapudi and Szalay (1998), the full series of catalogues yields results that are equivalent to a measurement with optimal weights in the full catalogue.

2.1 The PSCz Catalogue

PSCz is a redshift survey of all the IRAS galaxies in the Point Source Catalog that have a flux at $60\ \mu\text{m}$ greater than 0.6 Jy. With its 15,500 galaxies distributed over 84.1% of the sky, it constitutes the deepest and densest all-sky redshift survey to date. The median depth is just $8100\ \text{km s}^{-1}$,

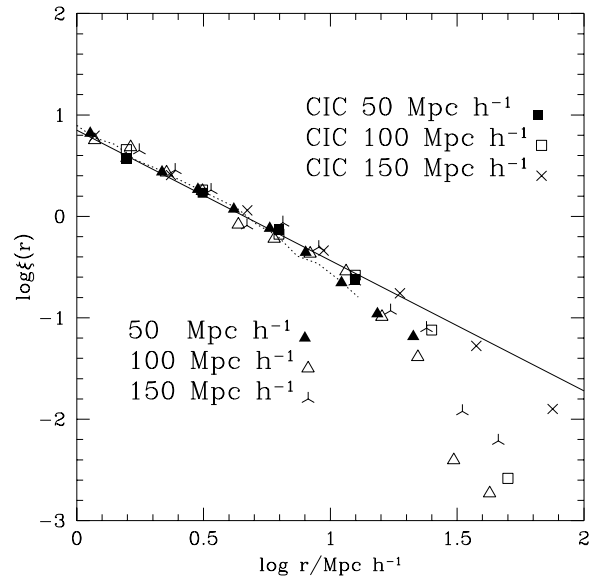


Figure 1. The two-point correlation function of the PSCz survey in redshift space. Three-sided symbols represent measurements using the Landy-Szalay estimator, while four-sided symbols show estimates derived from scaled counts-in-cells (c.f. §2.4). Results for three representative volume-limited subsamples are displayed. Statistical errorbars are typically smaller than the symbols (except on the largest scales), and are not plotted for clarity. The solid line is the fit by Fisher *et al.* (1994, see also Seaborne *et al.* 1999). The dotted line shows the predictions of the CDM model of Benson *et al.* (2000) for spiral galaxies.

although useful information is available out to $30,000\ \text{km s}^{-1}$ at high galactic latitudes and to $15,000\ \text{km s}^{-1}$ elsewhere. Full details of the survey may be found in Saunders *et al.* (2000). The analysis was restricted to the region of sky covered by the survey, with no attempt to interpolate the galaxy distribution within the masked areas (Branchini *et al.* 1999). Since the sample is relatively local, we can ignore evolutionary effects on the clustering and biasing.

2.2 Correlation Function

We estimate the two-point correlation function of the PSCz survey by means of the Landy and Szalay (1993; LS) estimator which has been shown to be optimal (Szapudi & Szalay 1998; Kerscher, Szapudi, & Szalay 1999). Denoting the number of data-data, data-random, and random-random pairs in a bin at distance r by DD , DR , and RR respectively, the definition of the estimator is

$$\hat{\xi}(r) = (DD - 2DR + RR)/RR. \quad (1)$$

For volume-limited surveys, uniform weighting yields minimum variance.

The three-sided symbols in Fig. 1 show our estimate for the PSCz two-point correlation function using the Landy-Szalay estimator on volume-limited samples of radii 50, 100, and $150h^{-1}$ Mpc. The square symbols show a different estimate based on the counts-in-cells (CIC) analysis described in §2.4. While a rigorous error calculation for the LS estimator is not available at present, errors for the CIC estimator can

be computed using the FORCE package (see §2.4). The $1-\sigma$ uncertainties are typically less than 5–7%, but grow rapidly at large separations, becoming 20–25% at $r \sim 25h^{-1}\text{Mpc}$ and larger beyond this. The LS and CIC estimators are only expected to agree in the regime where the correlation function is well approximated by a power-law regime. In this regime the uncertainties in both methods are most likely comparable. (The error bars have been omitted from the figure for clarity.) It is important to recognize that the data points in Fig. 1 (and in most other plots in this paper) are not independent and so the estimated errors cannot be used for maximum likelihood estimation without further analysis. This requires computing the cross-correlation matrix of all measurements, a complicated and ill-understood procedure which is beyond the scope of this letter.

Results for the remaining volume-limited subsamples are consistent with those displayed in the figure. For comparison, the solid line shows the fit of Fisher *et al.* (1994) to the correlation function of the IRAS 1.2-Jy survey, $\xi(r) = (r/r_0)^\gamma$, with $r_0 = 4.43h^{-1}\text{Mpc}$, and $\gamma = 1.28$. Our results are consistent with this fit, perhaps with a cut-off on large scales, as well as with the fit of Seaborn *et al.* (1999) to the full (flux-limited) PSCz survey. Since the deeper samples contain predominantly brighter galaxies, the similarity of the correlation functions in the subsamples suggests that any luminosity dependence of clustering is small. However, the different samples have galaxies in common and so their correlation functions are not independent. This weakens the sensitivity of this test for a luminosity dependence and so we prefer, instead, to use the mark correlations, as we now describe.

2.3 Luminosity Mark Correlation Function

The elegant tool of mark correlations, introduced into astrophysics by Beisbart and Kerscher (2000), is ideal for quantifying the luminosity dependence of clustering. If m_i denotes a mark, or a parameter characterizing a class of objects, the joint probability of finding a pair of galaxies at (m_1, r_1) and (m_2, r_2) , respectively is

$$\Gamma(m_1, m_2, r_1, r_2) dm_1 dm_2 d^3r_1 d^3r_2 \quad (2)$$

(see also Peebles 1980). If the mark is discrete, dm_1 is a Stieltjes-Lebesgue measure; otherwise it is the usual Lebesgue measure. The two-point correlation function is obtained by integration over the marginal distribution,

$$n^2 (1 + \xi(r)) = \int \Gamma dm_1 dm_2, \quad (3)$$

where $r = |r_1 - r_2|$. The conditional probability of finding a pair with marks m_1 and m_2 respectively is

$$P(m_1, m_2 | r) = \frac{\Gamma(m_1, m_2, r_1, r_2)}{n^2 (1 + \xi(r))}. \quad (4)$$

This quantity may be estimated from the catalogue as the ratio of all the pairs with the prescribed marks divided by all the pairs, both numbers taken at a given separation.

The luminosities were divided into luminosity quartiles, each of them containing equal numbers of galaxies. Thus, marks $m = 0, 1, 2, 3$ represent bins of increasing absolute luminosity. The rest of this subsection is exclusively concerned

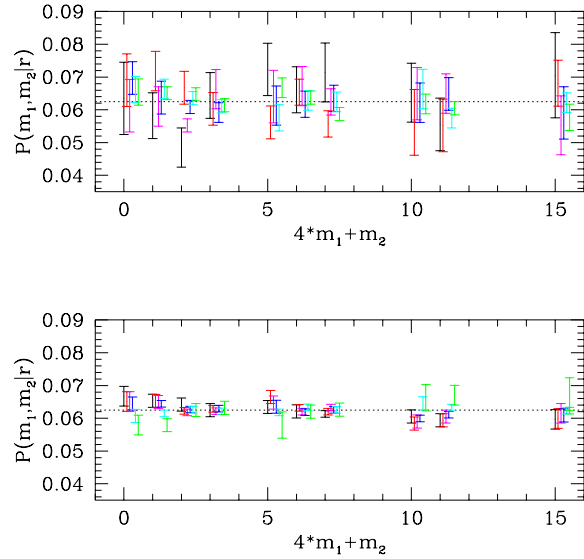


Figure 2. The conditional probability $P(m_1, m_2 | r)$. This is plotted as a function of $4m_1 + m_2$ (with $m_1 \geq m_2$) in order to separate the points. Here, $m_i = 0, 1, 2, 3$ represents the luminosity quartiles of a volume-limited PSCz subsample with radius of $50h^{-1}\text{Mpc}$, with the corresponding luminosity ranges between $(9.06 \cdot 10^{42}, 1.18233 \cdot 10^{43}, 1.64892 \cdot 10^{43}, 2.7935 \cdot 10^{43}, 4.2884 \cdot 10^{44})$ ergs/sec. For clarity, only symmetrical errorbars, estimated from a series of 10 realistic mock PSCz catalogues, are shown. Results for several scales are plotted, with small horizontal shifts to the right (for clarity), in increasing order: 2.35, 3.26, 4.51, 6.25, 8.67, 12.01 $h^{-1}\text{Mpc}$ (upper panel) and 16.64, 23.06, 31.94, 44.26, 61.32, 84.95 $h^{-1}\text{Mpc}$ (lower panel).

with the shallowest volume-limited subsample, cut at a distance of $50h^{-1}\text{Mpc}$, since this contains the largest range of luminosities. The same analysis was repeated for the other volume-limited subsamples with similar results.

The probability, $P(m_1, m_2 | r)$, is shown in Fig 2, as a function of $4m_1 + m_2, m_1 \geq m_2$ for a number of pair separations. For a particular pair (m_1, m_2) , results corresponding to increasing scales are slightly shifted towards the right for clarity and only symmetric errorbars are plotted. These were calculated from the dispersion of a set of 10 mock PSCz catalogues constructed from an N-body simulation by Cole *et al.* (1998) of a flat ΛCDM model, with cosmological constant, $\Lambda = 0.7$, and without any luminosity segregation. Fluxes were assigned randomly to galaxies to match the PSCz luminosity function and the various selection criteria discussed by Branchini *et al.* (1999) were applied in order to obtain realistic mock catalogues. For the smaller distances considered (upper panel), the errors agree with a naive Poissonian estimate, while for the larger scales (lower panel), the dispersion in the mock catalogues significantly exceeds the Poissonian expectation. Therefore, on small scales the dominant source of error is discreteness or shot noise, while on large scales finite volume effects are important.

The dotted line in Fig. 2 corresponds to the theoretical expectation for the probability, $p = (1/4)^2 = 0.0625$, for no correlation between the bins. Points above or below this line indicate a positive or negative correlation respectively. The results in Fig. 2 are consistent with no correlation on

any scale, for all pairs of marks. To quantify this statement, we use the 10 mock catalogues just mentioned. The formal χ^2 for all the points plotted, $\chi^2 = 0.381664$, would be unrealistically small for 120 independent points. However, the points in the figure are not independent because the normalization condition for $P(m_1, m_2 | r)$ requires the sum over all the bins to add up to unity. For this reason, the formal χ^2 has a non-standard distribution which can, in principle, be derived by Monte-Carlo methods using our mock catalogues. Although 10 mock catalogues are not sufficient to determine the distribution in detail, they allow us to reject a significant signal in Fig. 2: the χ^2 for the sample is close to the median for the simulations, 0.381914, whose highest and lowest 10 values are 0.204304 and 0.512983, respectively.

Our results agree with those from a similar, but independent, analysis of the PSCz survey by Kerscher and Beisbart (private communication). However, they disagree with preliminary results by Maddox *et al.* (in preparation) who, using different subsamples and statistical techniques, find a small but significant dependence of clustering on luminosity in the PSCz catalogue. Nevertheless, on the basis of analysis performed here, we may assume that any luminosity effects are sufficiently small that different volume-limited subsamples can be combined together to obtain minimum variance estimates of the higher order moments, as we do in the next section.

Before proceeding, we note that a comparative study of the IRAS 1.2 Jy and PSCz surveys by Teodoro *et al.* (1999) shows that the two density fields differ, within $\sim 80h^{-1}\text{Mpc}$, by a monopole term, a finding which is consistent with the spherical harmonics analysis of the PSCz survey by Tadros *et al.* (1999). Both these studies show that this apparent discrepancy disappears at a flux limit of 0.75 Jy. We have therefore repeated our analysis using samples limited at 0.75 Jy. Our results remain essentially unchanged for this sample, with a formal $\chi^2 = 0.468862$ for the comparison in Fig. 2.

2.4 Counts-in-Cells Analysis

We carried out a counts-in-cells analysis following the prescription developed by Szapudi *et al.* (1999). In a nutshell, we measured counts-in-cells using the successive convolution algorithm described in that paper, with a high rate of oversampling (up to 10^9 cells) on all scales for each volume-limited subsample. In practice, only about half of the cells intersected the geometry of the catalogue embedded in a cubic grid. From the counts-in-cells, the skewness and kurtosis were calculated using the method of Szapudi & Szalay (1993). This technique automatically corrects for shot noise by replacing moments with factorial moments. Thus, continuous definitions of the cumulants suffice:

$$S_N \equiv N^{N-2} Q_N = \frac{\langle \delta^N \rangle}{\xi^{N-1}}, \quad (5)$$

where δ denotes the field of density fluctuations, and $\bar{\xi} = \langle \delta^2 \rangle$ ($N = 3, 4$ for this paper). In the power-law approximation, the average correlation function is proportional to the correlation function. A Monte Carlo integration of the power-law fit to $\xi(r)$ given in the previous subsection yields $\bar{\xi}/2.4 = \xi$. We plot $\xi(r)$ derived from the first of equations (5) and this relation in Figure 1 (filled squares). The result is consistent with the direct estimate of $\xi(r)$ at pair

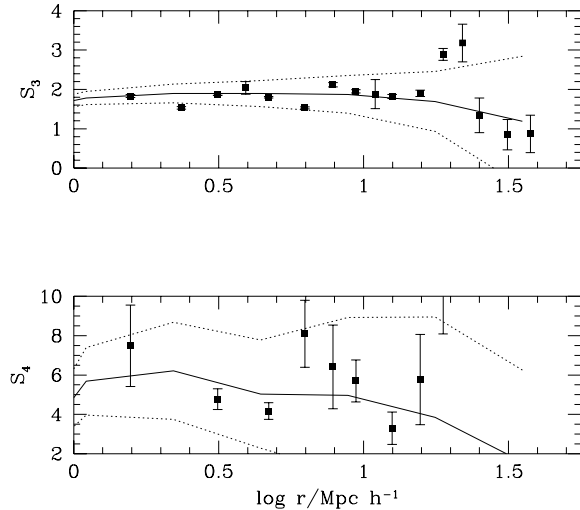


Figure 3. Near optimal composite measurements of S_3 (upper panel) and S_4 (lower panel). Different points can come from different volume-limited cuts, as detailed in Table 1. The errorbars were calculated using the SS model. The solid lines with the enveloping dotted lines representing the variance are the predictions of the semi-analytic model of galaxy formation of Benson *et al.* (1999) with the corresponding variance.

separations at which the power-law approximation is valid. For larger scales the above relation is no longer valid.

We determined the S_3 and S_4 for all the volume-limited subsamples and, for each cell-size, we cherry-picked the value with the smallest error. The analysis of the preceding sections suggests that any luminosity bias is small, so we can assume that the different volume-limited subsamples represent the same statistical process. Colombi *et al.* (1998) have shown that in these circumstances, selecting the highest signal-to-noise measurements from a series of volume-limited surveys is equivalent to the optimal minimum variance weighting of the flux-limited survey.

The errors were determined *ab initio* using the FORCE (FORtran for Cosmic Errors) package based on the theory of Szapudi & Colombi (1996), and Szapudi, Colombi & Bernardeau (1999). For each volume-limited subsample, the error was obtained for each order and scale under a range of plausible assumptions for the parameters involved. Whenever possible, these parameters were measured from the survey itself, such as its volume, the average number-counts and the variance in a cell. The variance over the survey volume was derived assuming the standard CDM power spectrum with $\Gamma = 0.5$ and $\sigma_8 = 1$. The higher order cumulants for $3 \leq S_3 \leq 8$ were calculated from perturbation theory with the effective index of the power spectrum $n = -0.5$. This yields slightly higher S_N s than are typically measured in the PSCz survey, thus providing a conservative overestimation of the (statistical) errors. Finally, the assumption of Szapudi & Szalay (1993, SS) was employed for the structure of cumulant correlators, the two point analogs of the Q_N s, namely $Q_{NM} = Q_N Q_M$ (see SS for details).

Table 1. Estimates of S_3 in cubic cells of size l . The errors, σ_{S_N} , were calculated using the FORCE package. The depth of the volume-limited subsample picked out by the near optimal procedure (see text) is denoted by R and given in $h^{-1}\text{Mpc}$. The value of R corresponding to each estimate of S_3 is also applicable to the corresponding estimate of S_4 , except for the case indicated by an *, for which $R = 50h^{-1}\text{Mpc}$ for S_4 .

l	S_3	σ_{S_3}	R	S_4	σ_{S_4}
0.78	2.77	0.35	50	-	-
1.57	1.83	0.04	50	7.49	2.07
2.35	1.53	0.03	75	-	-
3.14	1.87	0.02	50	4.77	0.53
3.92	2.04	0.16	125	-	-
4.71	1.80	0.02	75	4.17	0.42
6.27	1.53	0.02	100	8.09*	1.70
7.84	2.12	0.06	125	6.41	2.13
9.41	1.95	0.04	75	5.70	1.06
10.98	1.88	0.37	175	-	-
12.55	1.82	0.05	100	3.30	0.82
15.69	1.90	0.08	125	5.77	2.29
18.82	2.89	0.15	150	17.24	9.15
21.96	3.18	0.48	175	-	-
25.10	1.34	0.44	100	-	-
31.37	0.85	0.38	125	-	-
37.65	0.87	0.48	150	-	-

Provided that the parameters are well tuned, the calculations typically provide better than 50% accuracy for the statistical errors, normally a conservative overestimate as verified by Colombi *et al.* (1999) and Hoyle *et al.* (1999) from N-body simulations. It should, however, be borne in mind, that if the plausible guesses made for the parameters and models are grossly incorrect, or if systematic errors dominate, the theoretical error estimates might be inaccurate. We have varied some of the assumptions and parameter values within reasonable bounds without finding significant change. When the relative errors are approaching unity, the perturbative approach breaks down, but still indicates that the measurement has low significance. For more details of the method and its applicability see Szapudi *et al.* (1999). Note that these error estimates do not take into account cross-correlations or possible systematic errors and could therefore underestimate the true uncertainties.

3 DISCUSSION AND SUMMARY

We have characterized the clustering properties of galaxies in the PSCz survey of IRAS galaxies by means of the two-point correlation function, mark correlations, and the moments of counts-in-cells. Our two estimates of the correlation function, one based on a direct measurement and the other derived from counts-in-cells, are consistent with each other and agree well with previous measurements for IRAS galaxies (Moore *et al.* 1994, Fisher *et al.* 1994, Seaborne *et al.* 1999). Neither the correlation function itself nor the mark correlations show any significant evidence for a dependence of clustering on luminosity, over the limited range of luminosities probed by our volume-limited subsamples. Finally, we have firmly established that the skewness of the distribution of counts-in-cells in redshift space for IRAS galaxies has a value $S_3 \approx 2$.

Our estimated values of S_N , for $N = 3, 4$, are listed Table 1 and displayed in Fig. 3. The variation of these quantities over the range of scales probed by our analysis is small. Over the entire range, $S_3 = 1.89 \pm 0.62$ and $S_4 = 7.00 \pm 4.13$, while over the restricted range $1 - 20h^{-1}\text{Mpc}$, $S_3 = 1.93 \pm 0.35$. These results are in good agreement with previous analyses of counts-in-cells of IRAS galaxies, based on the QDOT survey (Saunders *et al.* 1993). For the parent catalogue of the 1.2Jy survey, Meiksin *et al.* (1992) obtained $S_3 = 2.2 \pm 0.2$ and $S_4 = 10 \pm 3$, while for the 1.2 Jy redshift survey itself Bouchet *et al.* (1993) found $S_3 = 1.5 \pm 0.5$ and $S_4 = 4.4 \pm 3.7$ and Fry & Gaztañaga (1994) derived $S_3 = 2.1 \pm 0.3$ and $S_4 = 7.5 \pm 2.1$. The significance of our study lies in the more densely sampled data set, the use of state-of-the-art measurement techniques, and a rigorous error calculation. All these features have enabled us to extend the dynamic range of previous studies and achieve unprecedented accuracy.

In contrast to the situation at optical wavelengths (see Hoyle *et al.* 1999 for an up-to-date discussion), the skewness of IRAS galaxies in redshift space agrees well with that in the parent, projected catalogue, as measured by Meiksin *et al.* (1992). Presently, these are the only datasets large enough to allow a measurement of S_3 with a precision better than 10% over a large dynamic range. The 2dF and SDSS surveys will enable estimates of S_3 with an error of only a few percent and of S_4 with an error of 10-25% over a large dynamic range (Szapudi *et al.* 1999). These surveys will clarify the role of redshift space and projection effects in the apparent disagreement between angular and 3D cumulants for optically selected galaxies, and enable a more direct comparison between the statistics of IRAS and optical galaxies.

In general, the flatness of the S_3 curve in redshift space is well understood from theoretical arguments, and supported by N-body simulations. Although the skewness rises to a non-linear plateau in real space, the random velocities associated with the 'finger of god' distortion in redshift space act as an effective smoothing. As a result, the S_3 curve remains flat in redshift space. Naturally, biasing complicates this picture inferred from simple theory and dark matter simulations. It is therefore perhaps surprising that S_3 should be so similar for IRAS and optically-selected samples since these have somewhat different spatial distributions. We speculate that this agreement is the result of a cancellation effect whereby the differences in spatial distribution are compensated for by differences in the strength of the redshift space distortions acting on each galaxy type.

To address the effects of biasing on statistical measurements of the galaxy distributions requires a detailed theory of galaxy formation. The solid line in Fig. 3. shows the predictions of the semi-analytic model of galaxy formation proposed by Cole *et al.* (2000) and Benson *et al.* (1999). According to the model, the higher order moments in *redshift space* for spiral galaxies are very similar to those for the galaxy population as a whole, although they differ in real space (Baugh, Szapudi, & Benson 2000). The predictions in the figure refer to spiral galaxies which, as a class, are a reasonable representation of IRAS galaxies. The dotted lines give the variance computed by varying the input parameters in the error estimation procedure. The agreement with the PSCz results is remarkably good. The shape of the S_3 and S_4 curves in the model reflects the kind of cancellation

effects mentioned above (see Baugh *et al.* 2000 and Hoyle *et al.* 1999 for further discussion). As shown in Fig. 1, the model predictions also agree well with the two-point correlation function of the PSCz survey. This model of galaxy formation assumes a flat, Λ -dominated CDM cosmology in which galaxies form by hierarchical clustering. The agreement with our results is the more remarkable since there are no adjustable parameters in the comparison, so that the theoretical lines in Figs. 1 and 3 are to be regarded as genuine predictions of the model.

Acknowledgments

We thank the rest of the PSCz team for use of the data before publication, S. Cole for providing mock PSCz catalogues and A. Benson and C. Baugh for providing theoretical predictions from the Durham semi-analytic model of galaxy formation and for useful comments. IS was supported by the PPARC rolling grant for Extragalactic Astronomy and Cosmology at Durham. CSF acknowledges a Leverhulme Research Fellowship. The FORCE (FORtran for Cosmic Errors) package is available from its authors, S. Colombi and IS (<http://www.cita.utoronto.ca/~szapudi/istvan.html>).

REFERENCES

- Benson, A., Baugh, C., Cole, S., Frenk, C.S. & Lacey, C. 1999, MNRAS, submitted (astro-ph/9910488)
 Baugh, C.M., Szapudi, I., Benson, A. 2000, in preparation
 Beisbart, C., Kerscher, M. 2000, ApJ, submitted (astro-ph/0001036)
 Bernardeau, F. 1994, ApJ, 433, 1
 Branchini E., *et al.* 1999, MNRAS, 308, 1
 Bouchet, F.R., *et al.* 1993, ApJ, 417, 36
 Cole, S., Hatton, S., Weinberg, D. & Frenk, C.S. 1998, MNRAS, 300, 945
 Cole, S., Lacey, C., Baugh, C. & Frenk, C.S. 1999, MNRAS, submitted.
 Colombi, S., Szapudi, I., Szalay, A.S., 1998, MNRAS, accepted (astro-ph/9711087)
 Efstathiou, G., *et al.* 1990, MNRAS, 247, 10
 Fischer *et al.* 1999 ApJ, submitted (astro-ph/9912119)
 Fisher, K.B., Davis, M., Strauss, M., Yahil, A., Huchra, J., 1994, MNRAS, 266, 50
 Fry, J. N. & Gaztañaga, E. 1994, ApJ, 425, 1
 Hoyle, F., Szapudi, I., & Baugh, C.M. 1999, submitted (astro-ph/9911351)
 Juszkiewicz, R., Bouchet, F. R., & Colombi, S. 1993, ApJ, 412, L9
 Kerscher, M., Szapudi, I. & Szalay, A. 1999, submitted (astro-ph/9912088)
 Landy, S.D., & Szalay, A. 1993, ApJ, 412, 64
 Meiksin, A., Szapudi, I., & Szalay, A., 1992, ApJ, 394, 87
 Moore, B., Frenk, C.S., Efstathiou, G. & Saunders, W., 1994, MNRAS, 269, 742
 Saunders *et al.* 2000, MNRAS, (submitted astro-ph/0001117)
 Seaborne *et al.* 1999, MNRAS, (accepted astro-ph/9905182)
 Szapudi, I., & Colombi, S. 1996, ApJ, 470, 131
 Szapudi, I., Colombi, S., Bernardeau, F., 1999, MNRAS, accepted
 Szapudi, I. & Szalay, A. 1993, ApJ, 408, 43 (SS)
 Szapudi, I. & Szalay, A. 1998, ApJ, 494, 41L
 Tadros, H. *et al.* 1999 MNRAS, 305, 527
 Teodoro, L. *et al.* 1999 MNRAS, submitted, (astro-ph/9908358).